Reflectance-based optically detected resonance studies of neutral and negatively charged donors in GaAs/$Al_xGa_{1-x}As$ quantum wells

G. Kioseoglou, H. D. Cheong, T. Yeo, H. A. Nickel, A. Petrou, and B. D. McCombe
Department of Physics and Center for Advanced Photonic and Electronic Materials, State University of New York at Buffalo, Buffalo, New York 14260

A. Yu. Sivachenko
The Weizmann Institute of Science, Rehovot 76100, Israel

A. B. Dzyubenko*
General Physics Institute, RAS, Moscow 117942, Russia

W. Schaff
Cornell University, Ithaca, New York, 14853
(Received 1 October 1999)

We report a reflectance-based optically detected resonance (ODR) study of neutral and negatively charged donors in GaAs/$Al_xGa_{1-x}As$ quantum-well structures. The intensity of the $e_1h_1(1s)$ excitonic reflectance feature was modulated by resonant absorption of a monochromatic far-infrared (FIR) laser beam. An externally applied magnetic field was used to bring the internal transitions among various impurity states in resonance with the FIR photon energy. Predicted, but not previously reported, internal transitions of negatively charged donors were observed and were found to be in good agreement with theoretical calculations. This study establishes that the reflectance-based ODR technique is a sensitive tool for the investigation of donor states (both neutral and negatively charged) in semiconductor quantum wells.

I. INTRODUCTION

Optically detected resonance (ODR) spectroscopy has proven to be a powerful method for the study of a variety of excitations in semiconductor systems such as cyclotron resonance,[1–4] internal transitions of both neutral and negatively charged donors,[5] internal transitions of neutral excitons,[6–9] and very recently, internal transitions of negatively charged excitons.[9] This technique monitors the intensity of the band-edge photoluminescence (PL) excited by a visible laser while the sample is simultaneously illuminated by a monochromatic far-infrared (FIR) laser beam. The energy levels of the system under study are tuned by an externally applied magnetic field. When the energy difference between two such states is brought into resonance with the FIR laser photon energy, a measurable change in the PL signal is generally observed. Optically detected resonance provides a number of advantages over more conventional FIR absorption. The first is high sensitivity, in part because the detection is in the visible spectrum where extremely efficient detectors are available, and in part because the PL is very sensitive to small changes in carrier distribution, even for very low densities of photoexcited carriers. The second advantage lies in the ability to monitor one of the many recombination channels for band-edge PL, e.g., neutral excitons, negatively charged excitons, impurity bound excitons, and impurity-to-band transitions. This spectroscopic specificity of ODR allows detailed investigation of the various mechanisms involved.

In the present work we focus on a study of GaAs/$Al_xGa_{1-x}As$ quantum wells using a variant of the usual ODR technique, reflectance-based ODR spectroscopy. The method consists of monitoring changes in the strength of the $e_1h_1(1s)$ excitonic reflectance feature induced by the FIR beam, rather than changes in the PL intensity. A strong modulation of the reflected light occurs when the FIR photon energy matches the energy difference between two electronic states of the system under appropriate circumstances. We will use the term ''reflectance-based optically detected resonance'' (RODR) for this technique. The more conventional ODR spectroscopy in which the interband PL intensity is monitored will be referred to as PLODR for the rest of the discussion. By comparing PLODR and RODR results from the same samples it was established that RODR is sensitive to both neutral and negatively charged donors. In addition, RODR spectra do not exhibit any internal excitonic transitions under the conditions of the experiment, i.e., in the absence of visible laser excitation. The RODR technique provides the following advantages: (a) Given its sensitivity to impurity states it can be used to help in the unambiguous identification of features in PLODR spectra in which both excitonic as well as impurity-related resonances are present. (b) Another advantage of RODR is that it decouples the signal level, i.e., the intensity of the reflected monochromatic light, from the number of photoexcited carriers in the wells. In PLODR experiments the intensity of the visible laser beam affects both the PL signal level and the carrier density and thus one cannot be varied without changing the other. Impurity states can be studied using RODR without the presence of photogenerated carriers that could at low densities cause broadening of the impurity-related transitions and at higher densities perturb the energy levels under

TABLE I. Sample parameters.

Sample	Well width (Å)	Barrier width (Å)	Periods	Doping
1	210	125	20	Doped with Si at $10^{16}\,cm^{-3}$ over the central 1/3 of the wells
2	125	150	30	Not intentionally doped
3	200	600	20	δ-doped with Si Well center: $2\times10^{10}\,cm^{-2}$ Barrier: $4\times10^{10}\,cm^{-2}$

study. (c) RODR allows the study of structures that do not have strong PL signals.

In the present work we demonstrate the utility of this technique by using RODR to investigate the electronic states of several $GaAs/Al_xGa_{1-x}As$ multiple-quantum-well (MQW) samples. The high sensitivity of RODR reveals new intradonor transitions of negative donor ions (D^-). These results are compared with theoretical calculations and found to be in good agreement.

II. EXPERIMENTAL

We have used three $GaAs/Al_xGa_{1-x}As$ quantum-well structures grown by molecular-beam epitaxy (MBE) in this study. Relevant parameters are listed in Table I. Sample 1 is doped with Si donors in the central 1/3 of the well layers. Sample 2 is not intentionally doped and exhibited strong intraexcitonic transitions in earlier PLODR studies.[6] Sample 3 is δ doped with Si donors in both the well centers and the barrier centers. The purpose of the barrier doping is to provide excess electrons in the wells so that the majority of the donors in the wells are negatively charged.[10–12] The RODR results from this sample are compared with those from previous FIR absorption and photoconductivity studies.[13] A schematic diagram of the setup for the RODR experiments is shown in Fig. 1. The samples were placed in an exchange gas system at 4.2 K in a 15/17 Tesla superconducting magnet cryostat. The combination of a 250-W broadband tungsten halogen lamp and a grating spectrometer was used to produce a tunable quasimonochromatic beam of light in the vicinity of the band gap of the $GaAs/Al_xGa_{1-x}As$ quantum-well structures. This beam was transmitted to the sample via a 600 μm diameter optical fiber oriented at a 30° angle with respect to the normal to the sample surface. A second fiber of the same dimensions placed at the same angle relative to the normal to the sample surface but at an azimuthal angle of 180° collected the reflected light and transmitted it to a Si-diode detector. Changes in the reflectance signal induced by the FIR laser beam were synchronously detected by a lock-in amplifier. Three FIR laser lines were used in these experiments: 70.6 μm (141.8 cm^{-1}), 96.5 μm (103.6 cm^{-1}), and 118.8 μm (84.2 cm^{-1}). The FIR laser beam was guided and focused onto the sample by a light pipe and condensing-cone system. A dedicated microcomputer adjusted the spectrometer wavelength so that the reflectance excitonic feature was tracked with a spectral window of approximately 5 cm^{-1} as the magnetic field was scanned from 0 to 15 tesla. The PLODR setup used for this work has been described elsewhere.[5] All PLODR spectra presented in this work were excited by the 632.8-nm line from a helium-neon laser; the corresponding photon energy (1.959 eV) lies above the band gap of both the GaAs and the $Al_xGa_{1-x}As$ layers of the structures under study.

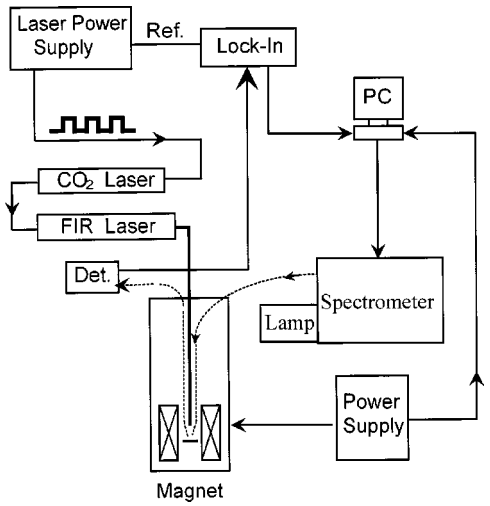

FIG. 1. Schematic diagram of setup for reflectance-based ODR experiments.

III. RESULTS AND DISCUSSION

The results are presented below for each of the three samples studied.

A. Sample 1

The reflectance spectrum from sample 1 at $B=2$ tesla is shown in Fig. 2(a). It contains features at 1516.3, 1525.9, 1528, and 1534.3 meV, which are identified as the bulk GaAs exciton, the $e_1h_1(1s)$, $e_1l_1(1s)$, and the $e_1h_1(2s)$ confined magnetoexcitons, respectively. The doubling of the e_1l_1 feature is due to the large spin splitting of the light holes induced by the magnetic field. In this experiment we monitored changes in the strength of the $e_1h_1(1s)$ excitonic feature induced by the FIR laser as the magnetic field was ramped. The choice of which energy is tracked within the line shape of the reflectance feature is important and will be discussed later.

A comparison between the PLODR and RODR spectra from sample 1 recorded with the 118.8-μm FIR laser line is shown in Fig. 3. The identification of the various features in

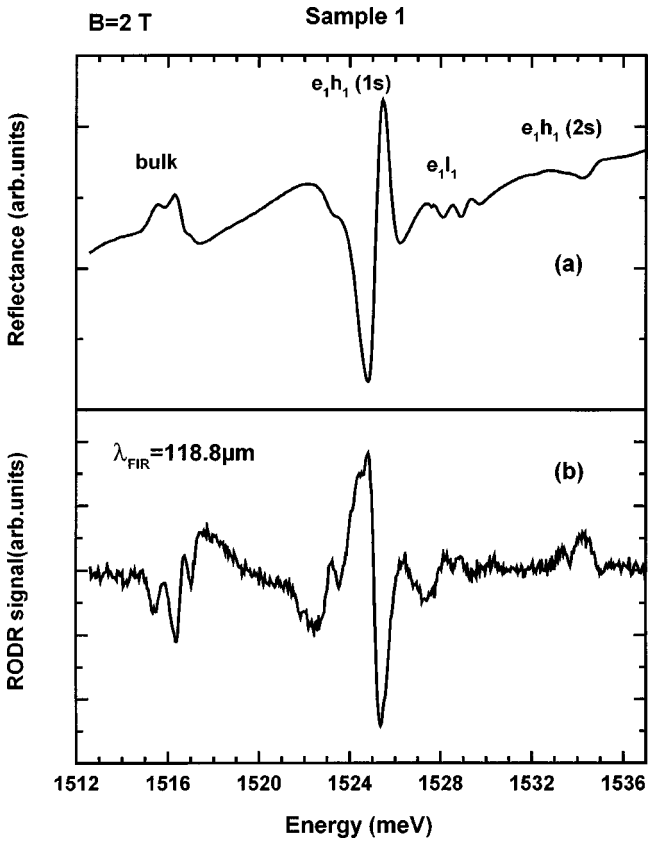

FIG. 2. (a) Reflectance spectrum from sample 1. (b) Changes in the reflectance signal plotted as a function of incident photon energy. Both spectra were recorded at $B=2$ tesla, at $T=4.2$ K and at a FIR wavelength of 118.8 μm.

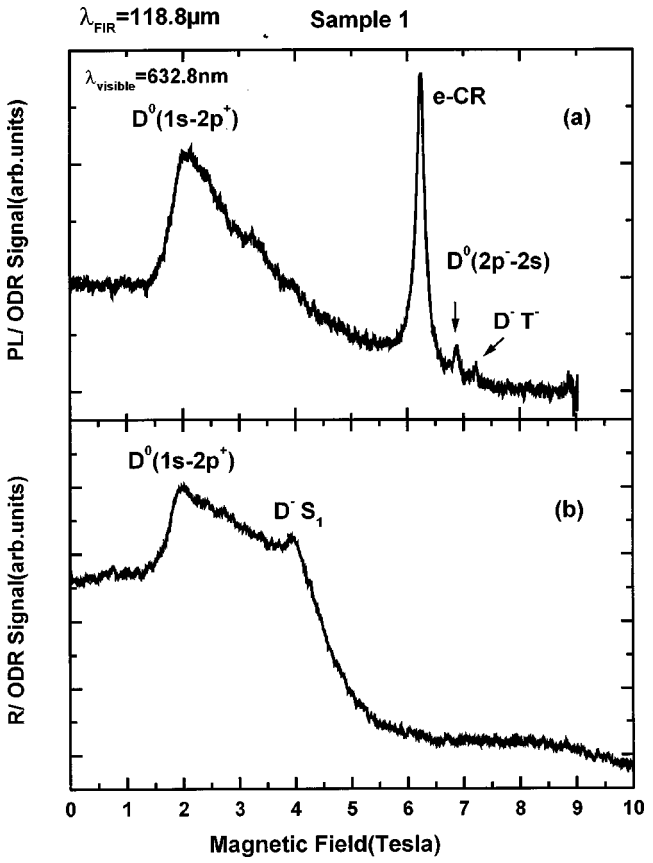

FIG. 3. ODR field sweeps from sample 1 at a FIR laser wavelength $\lambda_{FIR}=118.8\,\mu$m: (a) PLODR scan with excitation laser wavelength, $\lambda_{vis}=632.8$ nm; (b) RODR scan.

Fig. 3(a) was made on the basis of a comparison with FIR absorption measurements.[12–14] The dominant resonances in Fig. 3(a) are (1) the $1s$-$2p^+$ transition for neutral donors (D^0) at the well center at 2 tesla, and (2) the electron cyclotron resonance at 6.2 tesla. The hole cyclotron resonance is only observed for longer FIR wavelengths due to the much larger hole masses.[8] Two weaker features at 6.8 and 7.2 tesla were previously attributed to the $2p^-$-$2s$ transition of D^0 and the negatively charged donor (D^-) T^- (triplet) transition, respectively.[13] The labeling of the D^- transitions as well as the energy states involved are summarized in Table II. Here we follow the notation of Dzyubenko and Sivachenko[15] to identify the various states. The first quantum number $N=N_1+N_2$ is the total Landau-level quantum number (N_1 and N_2 are the Landau-level quantum numbers for each electron). The second quantum number $M=m_1+m_2$ is the total orbit-center quantum number (the total projection of the angular momentum $M_Z=N-M$). The third quantum number is the total spin and can have a value of either 1 or 0. The symbols S (for singlets) and T (for triplets) are used in this case. The D^- S_1 (singlet) transition in the PLODR spectrum appears as a very weak shoulder at 4 tesla.[12] The corresponding RODR spectrum of Fig. 3(b) contains the D^0 ($1s$-$2p^+$) and the D^- (S_1) transitions. We note that the D^- (S_1) transition is much stronger in the RODR spectrum and is clearly resolved. An additional broad RODR signal is observed between the D^0 ($1s$-$2p^+$) and D^- (S_1) distinct features. This could be due to unresolved internal transitions of donors redistributed away from the well center towards the barrier during growth. The weaker D^0 ($2p^-$-$2s$) and D^- (T^-) features in Fig. 3(a) were not observed in the RODR spectrum of Fig. 3(b).

Notably absent from the RODR spectrum is the electron cyclotron resonance, which is the strongest feature in the PLODR scan. This is expected since the PLODR spectrum was excited with the 632.8-nm line whose photon energy is above the band gaps of the GaAs and $Al_xGa_{1-x}As$ layers. As a result, a significant density of photoexcited electrons and holes is confined in the wells and thus contributes to a strong electron cyclotron signature. In contrast, the RODR spectrum is recorded under illumination by a very weak visible beam (power less than 1 μW) with photon energy equal to that of the exciton ground state. The weak D^0 ($2p^-$-$2s$) and D^- (T^-) features observed in PLODR for magnetic fields above the e-CR are also missing from the RODR spectra. This is expected because elevated carrier temperatures are required to populate the initial states of these two transitions. Exami-

TABLE II. Internal transitions of D^- (after Ref. 15).

Feature	Transition
S_1	$\|00S\rangle \rightarrow \|10S\rangle$
S_4	$\|00S\rangle \rightarrow \|12S\rangle$
S_x	$\|00S\rangle \rightarrow \|11S\rangle$
T^-	$\|01T\rangle \rightarrow \|11T\rangle$

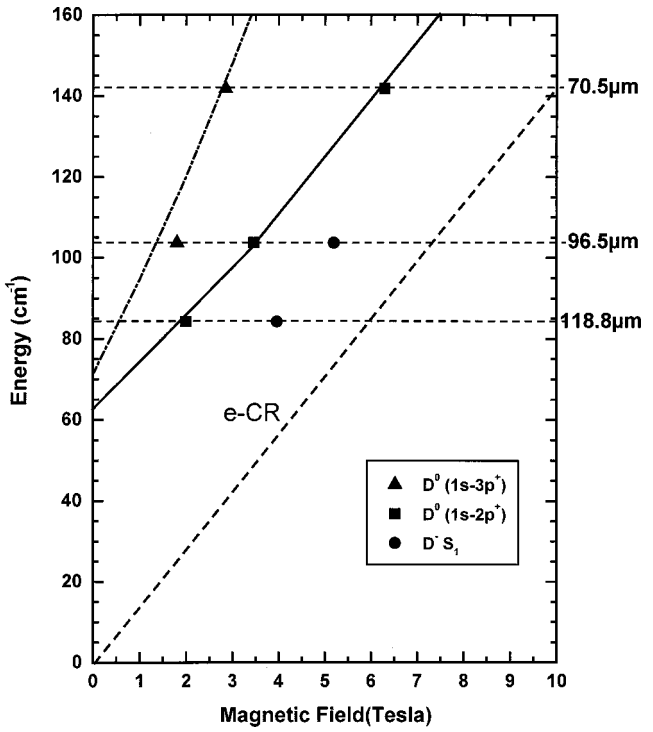

FIG. 4. Energies of the RODR resonances from sample 1 plotted as a function of magnetic field: squares, D^0 $(1s\text{-}2p^+)$; circles, D^- (S_1) transition; upright triangles, D^0 $(1s\text{-}3p^+)$. The dashed line represents the position of the electron cyclotron resonance. The solid (dot-dashed) line represents calculated values of the $1s\text{-}2p^+$ $(1s\text{-}3p^+)$ transition energy vs magnetic field.

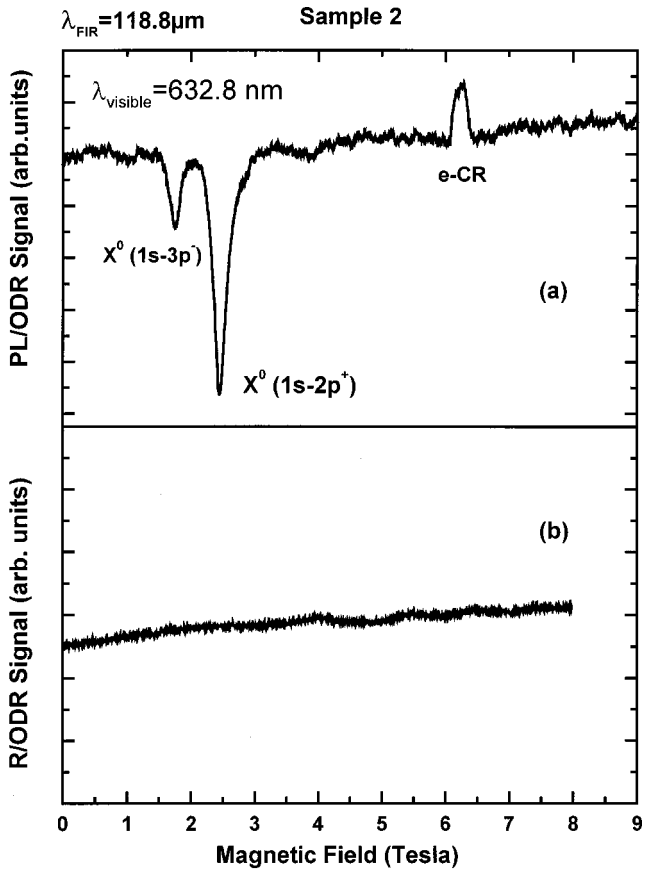

FIG. 5. ODR field sweeps from sample 2 at a FIR laser wavelength $\lambda_{FIR}=118.8\,\mu$m: (a) PLODR scan with excitation laser wavelength, $\lambda_{vis}=632.8$ nm; (b) RODR scan.

nation of the RODR scan in Fig. 3(b) raises the question of the origin of the excess electrons required for the formation of the D^- state. A plausible explanation is that a fraction of the donors ionize at the temperature of the experiment, and the resulting electrons are captured by other donors in the well to form D^- complexes (the two-electron singlet state has a lower total energy than the $D^0(1s)$ state plus a free electron). In other words the RODR spectrum of Fig. 3(b) requires the co-existence of neutral, ionized, and negatively charged donor impurities in the vicinity of the well center.

Once the magnetic field value B of a specific resonance is identified for a particular FIR wavelength, it is instructive to record a spectrum in which B is kept constant at B_r and the incident visible photon energy is scanned in the vicinity of the band gap. We shall refer to these spectra as ''energy scans.'' An example of such an energy scan from sample 1 under illumination by the 118.8-μm FIR laser line and the magnetic field B fixed at 2.0 tesla (i.e., at the $1s\text{-}2p^+$ resonance for D^0) is given in Fig. 2(b). Modulation of the reflectance signal is observed at the bulk exciton energy as well as at the energies of the $e_1h_1(1s)$ and $e_1h_1(2s)$ magnetoexcitons;[16] a weak modulation is observed at the position of the e_1l_1 exciton.

Below we discuss a possible mechanism responsible for the modulation of the reflectance intensity by the far-infrared photons. The changes in the exciton reflectance e_1h_1 feature is attributed to the resonant heating effect of the donors. As the donor effective temperature is increased via resonant absorption, a fraction of the donors is ionized and the wells become populated by a dilute electron gas. The presence of these electrons modifies the reflectance intensity resulting in a modulation of the excitonic reflectance feature. This was experimentally verified by recording two reflectance spectra $I_{R1}(\lambda)$ and $I_{R2}(\lambda)$ for two temperatures T_1 and T_2, respectively, at a fixed magnetic field resonant with the $1s\text{-}2p^+$ donor transition. The difference $\Delta I_R(\lambda)$ was numerically determined and was found to reproduce well the energy scans such as the one shown in Fig. 2(b).

The RODR signal at the bulk exciton probably comes from the buffer layer grown immediately before the quantum-well structure, and thus in close proximity to it. Resonant absorption by the donors in the wells results in an energy transfer from the FIR radiation field to the quantum wells and then to the buffer. This absorbed energy is probably transferred to the buffer via phonons and results in the observed modulation of the bulk exciton feature intensity.

In all of this work we collected data by tracking a particular point of the complicated $e_1h_1(1s)$ line shape. This point was chosen so as to maximize the RODR signal.

A summary of the RODR results on sample 1 is given in Fig. 4 in which we plot the energies of the observed resonances as function of magnetic field. The dashed line represents the electron cyclotron energy. The solid (dot-dashed) line represents a calculation of the $1s\text{-}2p^+$ $(1s\text{-}3p^+)$ transition energies for the neutral donors[17,18] as a function of the magnetic field. The experimental results for the neutral donors are in good agreement with the calculations. The results for the negatively charged donors will be discussed in detail in Sec. III C.

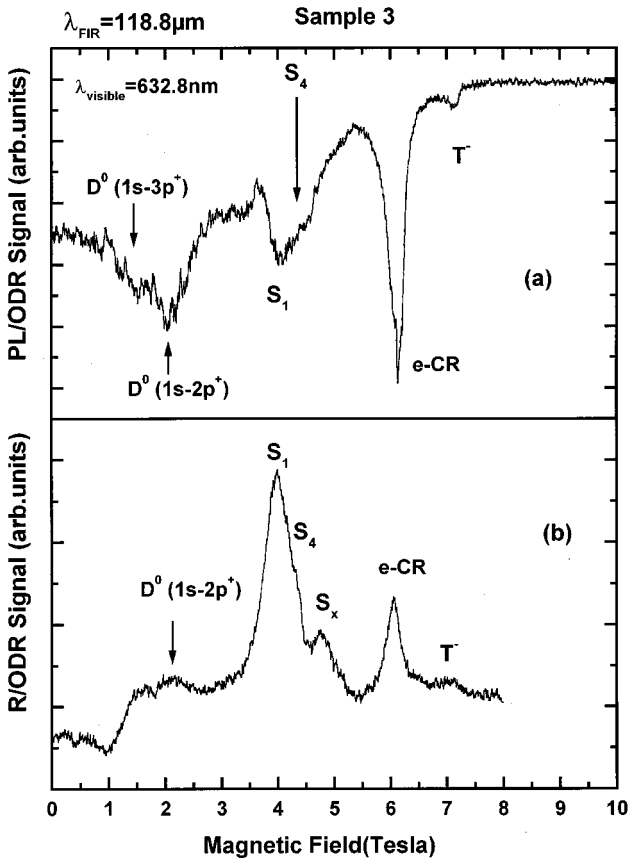

FIG. 6. ODR field sweeps from sample 3 at a FIR laser wavelength, $\lambda_{FIR}=118.8\,\mu$m: (a) PLODR scan at an excitation laser wavelength $\lambda_{vis}=632.8$ nm, (b) RODR scan.

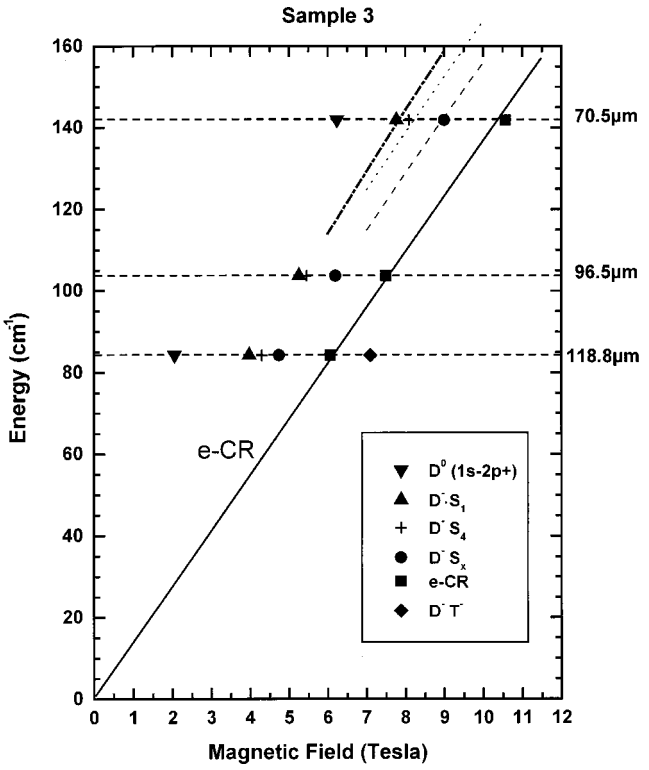

FIG. 7. Energies of the RODR resonances from sample 3 plotted as a function of magnetic field: diamonds, D^- (T^-); squares, electron cyclotron resonance; circles, D^- (S_x); crosses, $D^-(S_4)$; upright triangles, D^- (S_1); inverted triangles, D^0 $(1s\text{-}2p^+)$ transition. The solid line is the calculated value for electron cyclotron resonance; the dot-dashed, dotted, and dashed lines represent calculated values for the $D^-(S_1)$, $D^-(S_4)$, and $D^-(S_x)$ transitions, respectively.

B. Sample 2

In Fig. 5 we present the PLODR and RODR spectra from sample 2 recorded with the 118.8-μm FIR laser line. The PLODR spectrum of Fig. 5(a) in addition to the electron cyclotron resonance at 6.2 tesla exhibits two other sharp resonances at 1.75 and 2.45 tesla. These have been attributed to the $X^0(1s\text{-}3p^-)$ and $X^0(1s\text{-}2p^+)$ internal transitions of the exciton.[6,8] In contrast, the RODR spectrum of Fig. 5(b) shows no observable resonance for the same magnetic field range. No impurity features are present because sample 2 is not intentionally doped, and residual impurities are present in very low densities. The electron cyclotron resonance is absent because unlike PLODR the RODR experiments do not require excitation with a visible laser beam that results in a significant density of photogenerated carriers in the wells. The number of excitons created by the quasimonochromatic visible beam in the RODR experiments is not adequate to cause enough absorption of the FIR radiation to be observed as a change in the reflectance signal. Thus, while RODR spectroscopy is quite sensitive to the presence of impurities in the wells, it does not respond to the low density of photoexcited excitons (total sheet density estimated to be less than $2\times10^5\,\mathrm{cm}^{-2}$/well) and thus can be used to differentiate excitonic from impurity-related transitions in some cases.

C. Sample 3

The PLODR and RODR scans from sample 3 recorded with the 118.8-μm laser line are shown in Figs. 6(a) and 6(b), respectively. Sample 3 is δ doped in both the well centers and the barrier centers (see Table I). The barrier donors result in excess electrons in the wells that can bind to a fraction of the neutral well donors and form the negatively charged donor (D^-) complex.[10–12] Both ODR spectra are quite complicated because they contain features associated with neutral (D^0) and negatively charged (D^-) donors, as well as electron cyclotron resonance. The D^0 $(1s\text{-}2p^+)$ and the D^0 $(1s\text{-}3p^+)$ transitions are observed at 2 and 1.4 tesla, respectively. Electron cyclotron resonance occurs at 6.2 tesla. In contrast to sample 1 this resonance now appears in the RODR spectrum. This is attributed to the fact that sample 3 is modulation doped, and therefore the wells in this structure are populated by a substantial density of excess electrons (approximately $1\times10^{10}\,\mathrm{cm}^{-2}$ per well) originating from the barrier donors. The features associated with the D^- states in Fig. 6(b) are stronger compared to those in Fig. 6(a) and as a result more details can be discerned from the RODR spectra. As in the case of sample 1, we label the various D^- internal transitions with the notation of Ref. 15. In addition to the S_1 and T^- features observed in sample 1, the PLODR and RODR spectra contain S_4 at 4.3 tesla and S_x at 4.8 tesla. The feature S_4 corresponds to the $|00S\rangle\rightarrow|12S\rangle$ transition.[15] Its position agrees well with recent calculations.[19] The position of S_x agrees with that calculated for the $|00S\rangle\rightarrow|11S\rangle$ resonance. We note that this transition violates the $\Delta M_z=\pm1$ selection rule ($\Delta M_z=0$ for this transition) valid for

the Faraday geometry. It is possible that this is due to the fact that the FIR beam is not very well collimated and therefore the $\Delta M_z = \pm 1$ rule is relaxed. This assumption cannot explain the observation of the $|00S\rangle \rightarrow |11S\rangle$ transition because a FIR photon with nonzero polarization in the z direction must change the parity of the confinement envelope function. There are two possible explanations for the S_x feature. Either the agreement with the calculated value of the $|00S\rangle \rightarrow |11S\rangle$ transition is fortuitous or there is a symmetry-breaking mechanism which is not currently understood.

In Fig. 7 we present a summary of the RODR results from sample 3 by plotting the energies of the observed resonances as a function of magnetic field and compare them with calculated values in the high-field limit. In this summary we concentrate on the D^--related features. The calculated energy of the $D^-(S_1)$ transition[20] is plotted by the dot-dashed line. As seen from the plot, the experimental point for S_1 at 70.5 μm is in reasonable agreement with the calculation. The other D^--related transitions (i.e., S_4 and S_x) at 70.5 μm also agree with the calculations.[19] The dotted (dashed) line in Fig. 7 represents the calculated values for the S_4 (S_x) D^- transitions.

IV. CONCLUSIONS

We have presented a reflectance-based ODR study of neutral (D^0) and negatively charged (D^-) donors in GaAs/Al_xGa_{1-x}As quantum-well structures. The experiments were carried out by monitoring changes in the reflectance intensity of the $e_1h_1(1s)$ exciton induced by a monochromatic FIR laser beam under resonant conditions. Resonance was achieved by applying an external magnetic field which tuned the energies of the donor internal transitions through the FIR photon energies. The results from RODR spectroscopy were compared with those from the more conventional PLODR. The RODR technique is found to be sensitive to internal transitions of neutral and negatively charged donors that are present in the samples. In modulation-doped heterostructures for which there are substantial excess free electrons, the electron cyclotron resonance has a signature in the RODR spectra. Under the conditions of these experiments, in which (unlike the PLODR method) no above-gap illumination was used, the exciton internal transitions were not observed due to the very low photoexcited exciton density. In comparison with PLODR spectroscopy reflectance-based ODR offers the following advantages: (a) it can be used to differentiate unambiguously between impurity- and exciton-related transitions, which appear in roughly equal strength in the PLODR spectra. (b) RODR experiments are carried out in the absence of a significant density of photogenerated carriers in the wells, which may perturb the energy states under study. (c) Systems which do not exhibit strong PL can be studied by RODR. In combination with the more conventional PLODR technique, RODR is a powerful tool for the investigation of various impurity-related FIR excitations in semiconductor heterostructures.

ACKNOWLEDGMENTS

A.B.D. is grateful to the Humboldt Foundation for research support. This work was supported by NSF Grant No. DMR 9722625.

*Present address: Institut für Theoretische Physik, J. W. Goethe-Universität, 60054 Frankfurt, Germany.

[1] M. G. Wright, N. Ahmed, A. Koohian, K. Mitchell, G. R. Johnson, B. C. Cavenett, C. R. Pidgeon, C. R. Stanley, and A. H. Kean, Semicond. Sci. Technol. **5**, 438 (1990).

[2] S. I. Gubarev, A. A. Dremin, I. V. Kukushkin, A. V. Malyavkin, M. G. Tyazhlov, and K. von Klitzing, Pis'ma Zh. Eksp. Teor. Fiz. **54**, 361 (1991) [JETP Lett. **54**, 355 (1991)].

[3] C. Wetzel, Al. L. Efros, A. Moll, B. K. Meyer, P. Omling, and P. Sobkowicz, Phys. Rev. B **45**, 14 052 (1992).

[4] R. J. Warburton, J. G. Michels, R. J. Nicholas, J. J. Harris, and C. T. Fox, Phys. Rev. B **46**, 13 394 (1992).

[5] J. Kono, S. T. Lee, M. S. Salib, G. S. Herold, A. Petrou, and B. D. McCombe, Phys. Rev. B **52**, R8654 (1995).

[6] M. S. Salib, H. A. Nickel, G. S. Herold, A. Petrou, B. D. McCombe, R. Chen, K. K. Bajaj, and W. Schaff, Phys. Rev. Lett. **77**, 1135 (1996).

[7] J. Černe, J. Kono, M. S. Sherwin, M. Sundaram, A. C. Gossard, and G. E. W. Bauer, Phys. Rev. Lett. **77**, 1131 (1996).

[8] H. A. Nickel, G. S. Herold, M. S. Salib, G. Kioseoglou, A. Petrou, B. D. McCombe, and D. Broido, Physica B **249**, 598 (1998).

[9] H. A. Nickel, G. S. Herold, T. Yeo, G. Kioseoglou, Z. X. Jiang, B. D. McCombe, A. Petrou, D. Broido, and W. Schaff, Phys. Status Solidi B **210**, 341 (1998).

[10] S. Huant, S. P. Najda, and B. Etienne, Phys. Rev. Lett. **65**, 1486 (1990).

[11] E. R. Mueller, D. M. Larsen, J. Waldman, and W. D. Goodhue, Phys. Rev. Lett. **68**, 2204 (1992).

[12] S. Holmes, J. P. Cheng, B. D. McCombe, and W. Schaff, Phys. Rev. Lett. **69**, 2571 (1992).

[13] S. R. Ryu, Z. X. Jiang, W. J. Li, B. D. McCombe, and W. Schaff, Phys. Rev. B **54**, R11 086 (1996).

[14] N. C. Jarosik, B. D. McCombe, B. V. Shanabrook, J. Comas, J. Ralston, and G. Wicks, Phys. Rev. Lett. **54**, 1283 (1985).

[15] A. B. Dzyubenko and A. Yu. Sivachenko, Phys. Rev. B **48**, 14 690 (1993).

[16] G. Duggan, Phys. Rev. B **37**, 2759 (1988).

[17] R. L. Greene and K. K. Bajaj, Phys. Rev. B **31**, 913 (1985).

[18] R. Chen, J. P. Cheng, D. L. Lin, B. D. McCombe, and T. F. George, J. Phys.: Condens. Matter **7**, 3577 (1995).

[19] A. Yu. Sivachenko and A. B. Dzyubenko (unpublished).

[20] A. B. Dzyubenko, A. Mandray, S. Huant, A. Yu. Sivachenko, and B. Etienne, Phys. Rev. B **50**, 4687 (1994).